Energy & Environmental Science

Cite this: DOI: 10.1039/c0ee00326c

www.rsc.org/ees

PAPER

High oxygen-reduction activity and durability of nitrogen-doped graphene

Dongsheng Geng,[a] Ying Chen,[a] Yougui Chen,[a] Yongliang Li,[a] Ruying Li,[a] Xueliang Sun,*[a] Siyu Ye[b] and Shanna Knights[b]

Received 30th July 2010, Accepted 13th December 2010
DOI: 10.1039/c0ee00326c

Nitrogen-doped graphene as a metal-free catalyst for oxygen reduction was synthesized by heat-treatment of graphene using ammonia. It was found that the optimum temperature was 900 °C. The resulting catalyst had a very high oxygen reduction reaction (ORR) activity through a four-electron transfer process in oxygen-saturated 0.1 M KOH. Most importantly, the electrocatalytic activity and durability of this material are comparable or better than the commercial Pt/C (loading: 4.85 μg_{Pt} cm^{-2}). XPS characterization of these catalysts was tested to identify the active N species for ORR.

1. Introduction

Both fuel cells, for power generation, and metal–air batteries, for energy storage, require an efficient electrode for oxygen reduction reaction (ORR). Such electrodes are usually carbon-supported platinum electrodes that are used to catalyze four-electron oxygen reduction to water. However, the kinetics of ORR is sluggish, even on pure Pt. Also, Pt particles dissolve and agglomerate over time, which diminishes the performance of fuel cells. Combined with the performance durability problems, the high cost of Pt, due to its low abundance in nature, hinders the commercial viability of fuel cells. The search for cheap, stable and more active electrocatalysts for ORR is thus of great importance.

Along with recent intense research efforts in reducing or replacing Pt-based catalysts in fuel cells,[1–4] it has been found that nitrogen-doped carbon materials (especially, vertically aligned nitrogen-containing carbon nanotubes, nitrogen doped ordered mesoporous graphitic carbon, and silk-derived carbon (0.8% nitrogen in the carbon network)) could act as effective metal-free electrocatalysts.[5–11] Although the real active site of nitrogen-doped carbon materials remains unclear, in general, it has been believed that the doped nitrogen atoms (such as graphite-like, pyridine-like, pyrrole-like, and quaternary nitrogen atoms) play a crucial role for ORR.[11–13] Graphene, on the other hand, a new and 2-dimensional carbon material, has recently attracted great interests for both fundamental science and applied research.[14–18] It has not only high surface area, and excellent conductivity, but also unique graphitic basal plane structure that should guarantee its durability. It is well known that the greater the extent of graphitization of the carbon material, the greater the durability it has.[19] The unique properties of nitrogen-doped carbon materials and graphene promoted us to investigate the ORR activity of nitrogen-doped graphene. Although nitrogen-doped graphene has been shown very recently to have high electrocatalytic activity and long-term operation stability for the ORR,[20] the exact extent of the electrocatalytic activity of this material remains unknown, perhaps due to the limitation of the chemical

[a]*Department of Mechanical and Materials Engineering, University of Western Ontario, 1151 Richmond Street N., London, Ontario, Canada N6A 5B9. E-mail: xsun@eng.uwo.ca; Fax: +1-519-6613020; Tel: +1-519-6612111, ext. 87759*
[b]*Ballard Power Systems Inc., 9000 Glenlyon Parkway, Burnaby, BC, Canada V5J 5J8*

Broader context

Energy shortages and environmental pollution are serious challenges that humanity will face for the long-term. Proton Exchange Membrane Fuel cells (PEMFCs) are non-polluting and efficient energy conversion devices that are expected to play a dominant role in future energy solutions. However, the current PEMFCs system still faces significant technological roadblocks which have to be overcome before the system can become economically viable. A major impediment to the commercialization of PEMFC is the high cost and stability of Pt-based electrocatalysts. Thus, one of the important challenges is the development of platinum-free catalysts. Nitrogen-doped carbon materials as the metal-free catalysts have recently been found to exhibit high catalytic activity for oxygen reduction reaction in fuel cell. Graphene, a new-type and two-dimensional (one-atom-thickness) allotrope of carbon with a planar honeycomb lattice, has attracted great interests for both fundamental science and applied research due to its various remarkable properties. Here, we present that nitrogen-doped graphene can be synthesized easily at a large scale and it has the comparable or better activity and stability than the commercial Pt/C (loading: 4.85 μg_{Pt} cm^{-2}) towards oxygen reduction reaction.

vapour deposition (CVD) preparation method used. The CVD method only made a graphene film on a surface of Ni-coated SiO_2/Si wafer. It is very difficult to scale up, which will inevitably limit the wide use as practical electrodes of N-graphene. And it appears impossible to fabricate membrane electrode assembly (MEA) for fuel cells based on the method. In this work, we prepare nitrogen-doped graphene at a large scale, and provide a detailed comparison to commercial Pt/C (E-TEK) as catalysts for ORR.

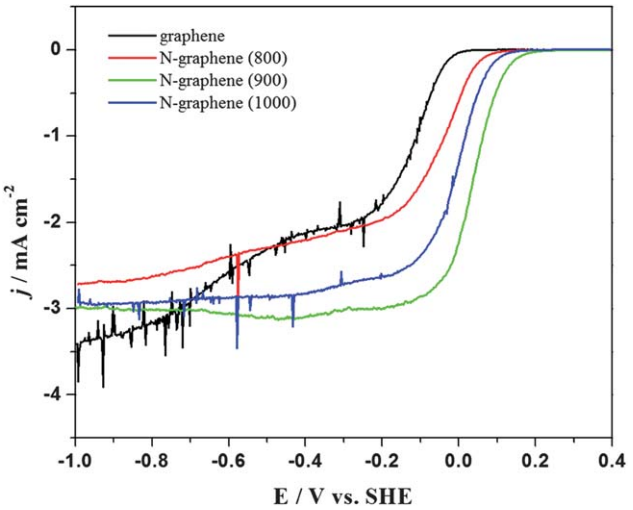

Fig. 1 The linear-sweep voltammograms of graphene and N-graphene under different temperatures. Electrolyte: O_2-saturated 0.1 M KOH, scan rate: 5 mV s^{-1}, and rotation speed: 1600 rpm.

2. Experimental

Natural flake graphite (Aldrich, +100 mesh) was used as the starting material. Graphene was first prepared by the oxidation of the natural flake graphite using the Staudemaier method followed by the heat-treatment at 1050 °C for 30 s.[21] The nitrogen-doped graphene was obtained by heating under high purity ammonia mixed with Ar at 800 °C (N-graphene (800)), 900 °C (N-graphene (900)), and 1000 °C (N-graphene (1000)).[22]

The ORR activity of nitrogen-doped graphenes was evaluated in 0.1 M KOH solution with a rotating ring-disk electrode (RRDE) equipment. Platinum wire and Hg/HgO (20% KOH) electrode were used as the counter and the reference electrode, respectively. The potentials presented in this study are referred to as standard hydrogen electrode (SHE). The potential is 0.098 V *versus* SHE with respect to the electrodes Hg/HgO. The working electrode was prepared by the thin-film electrode method. Briefly, 5 mg of N-graphene was dispersed in the solution (1080 μL ethanol and 180 μL of 5 wt% Nafion) and ultrasonically blended for 30 min. 10 μL of this suspension (loading: 160 μg cm^{-2}) was dropped on the disk electrode. Cyclic voltammograms (CVs) were recorded by scanning the disk potential from 0.4 to −1.0 V *vs.* SHE at a scan rate of 5 mV s^{-1}. And the ring potential was maintained at 0.7 V *vs.* SHE in order to oxidize any hydrogen peroxide produced. First, CVs were recorded at 5 mV s^{-1} using nitrogen atmosphere to obtain the background

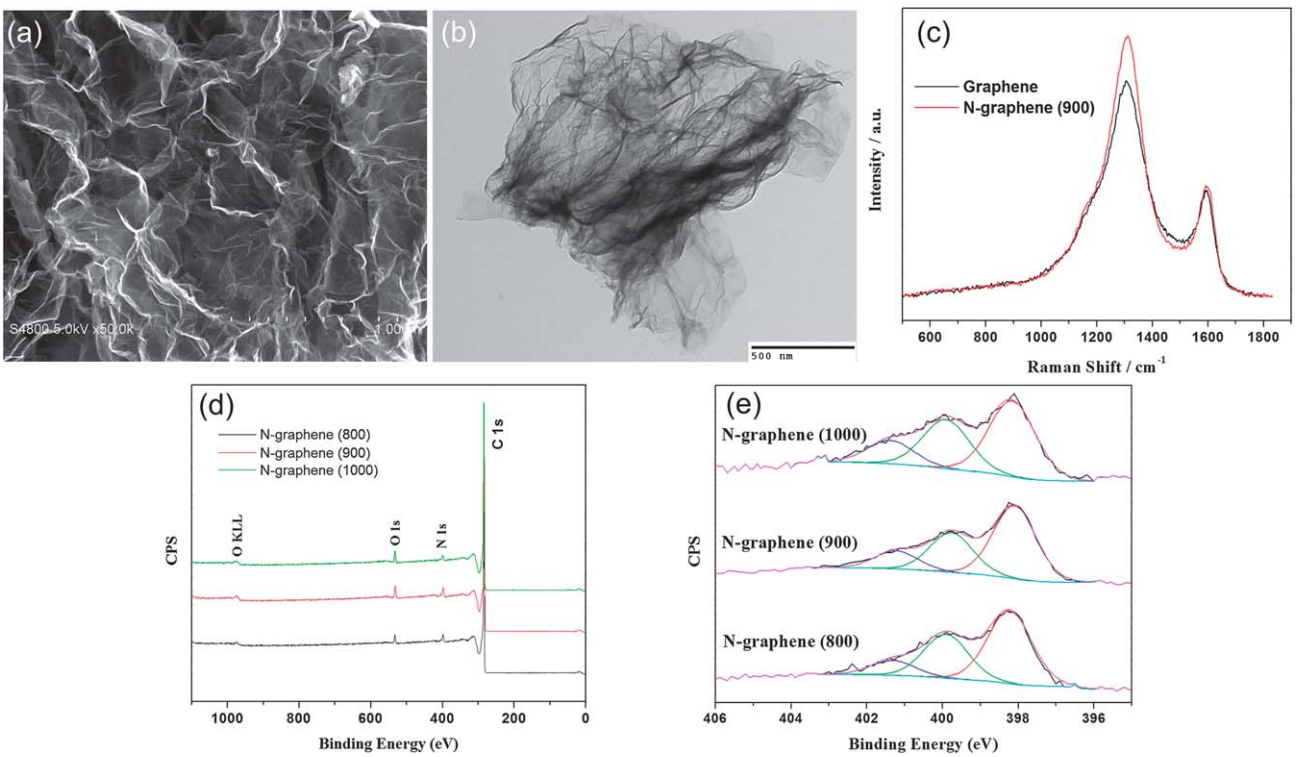

Fig. 2 The typical SEM (a) and TEM (b) images for N-graphene (900). (c) The Raman spectrum of graphene and N-graphene (900). (d) The XPS survey for three samples; (e) the high-resolution N1s spectrum for N-graphene: the black and purple lines are the raw and fitted spectra; the red, green, and blue lines correspond to pyridine-like N (398.1 eV), pyrrole-like N (399.9 eV), and quaternary N (401.3 eV), respectively.

Table 1 Distribution of N species obtained from the de-convolution of the N1s peaks by XPS

Sample	N content (at%)	Pyridine-like (398.1 eV, at%)	Pyrrole-like (399.9 eV, at%)	Quaternary (401.3 eV, at%)
N-Graphene (800)	2.8	1.5455	0.9352	0.3192
N-Graphene (900)	2.8	1.5596	0.8484	0.3892
N-Graphene (1000)	2.0	1.022	0.662	0.316

capacitive currents. Next, the CVs were recorded using the oxygen-saturated electrolyte. The electrolyte solution was purged with oxygen for 30 min before commencing oxygen reduction on the disk electrode.

3. Results and discussion

Fig. 1 shows the linear-sweep voltammograms in O_2-saturated 0.1 M KOH of graphene and graphene treated by ammonia at various temperatures. N-graphene (900) was shown to have a considerably higher activity toward ORR than the other materials. It has high onset potential for ORR (E_{ORR}) and a well-defined limiting current plateau. The values of onset potential for ORR (E_{ORR}) for graphene, N-graphene (800), N-graphene (900), and N-graphene (1000) were 0.046, 0.184, 0.308, and 0.204 V, respectively. Obviously, the ORR activity of N-graphene is strongly dependent on the heat treatment temperature and the optimum temperature appears to be 900 °C. Although the catalyst roughness effect cannot be completely excluded, we do not think that it is the major effect on the ORR activity. This conclusion has been obtained in our recent work.[23] By comparing the onset potential of glassy carbon and graphene, it has been revealed that they have similar activity although graphene has the higher roughness factor than the polished glassy carbon electrode. Generally, it has been believed that the nitrogen content and N species proportion in the carbon materials play a key role for the improved activity.[6,9] It is thus interesting to investigate the difference in nitrogen content and N species proportion of these ammonia-treated graphenes as a function of heat-treatment temperature. Fig. 2a and b show the typical SEM

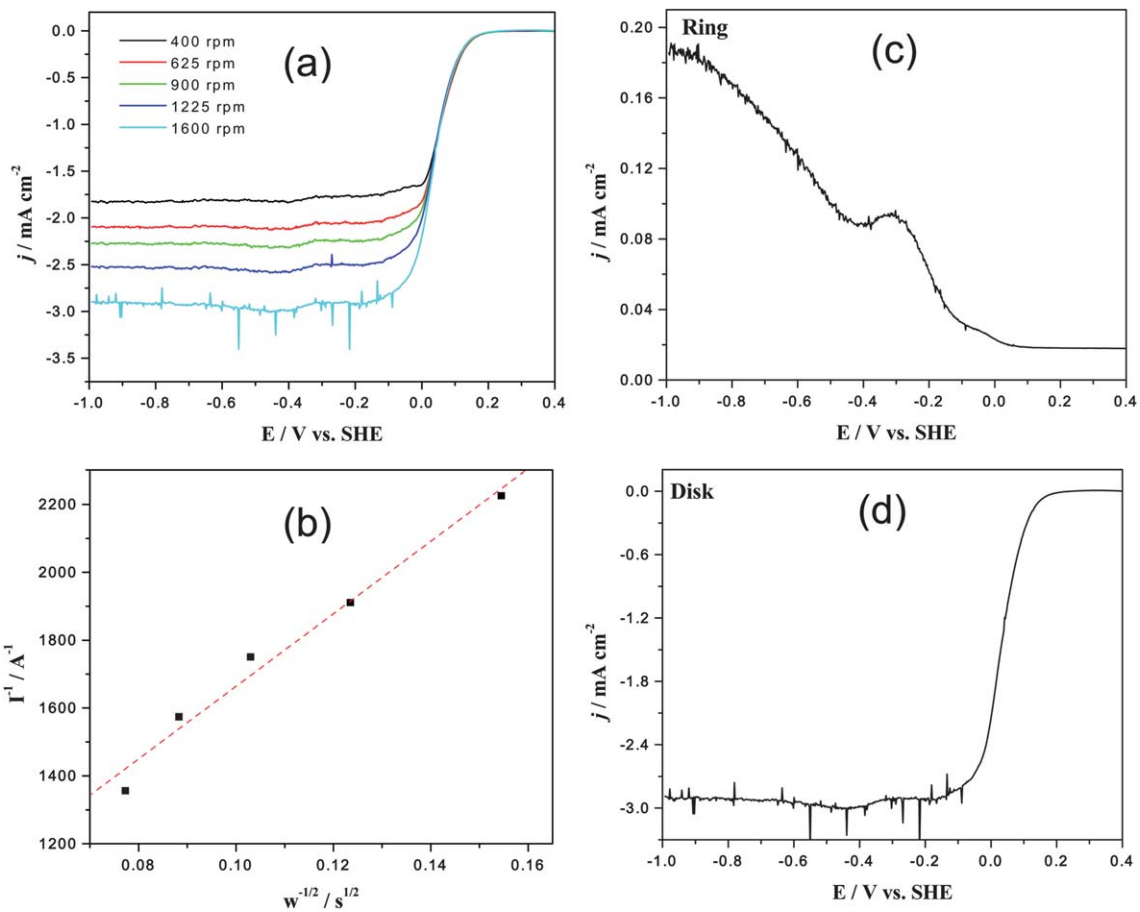

Fig. 3 (a) Measured ORR currents of N-graphene (900) catalyst at different electrode rotation speeds and (b) Koutecký–Levich plot at −0.5 V using the data obtained from (a). (c and d) The current density of ring and disk measured by RRDE for N-graphene (900). Scan rate: 5 mV s^{-1}, electrolyte: 0.1 M KOH.

and TEM images of N-graphene. It can be seen that the material is transparent with a voile-like structure. Meanwhile, from the Raman spectra shown here (Fig. 2c), it can be known that the D band, observed at approximately 1310 cm^{-1}, is disorder induced. It is attributed to structural defects on the graphitic plane. The G band, observed at approximately 1583 cm^{-1}, is commonly observed for all graphitic structures and attributed to the E2g vibrational mode present in the sp^2 bonded graphitic carbons. The intensity ratio of the first peak to the second peak, namely the I_D/I_G ratio, provides the indication of the amount of structural defects and a quantitative measure of edge plane exposure. N-graphene was found to have the higher I_D/I_G ratio of 2.25, obviously larger than 1.97 observed for graphene. The larger I_D/I_G ratio observed for N-graphene is a result of the structural defects and edge plane exposure caused by heterogeneous nitrogen atom incorporation into the graphene layers. Furthermore, XPS characterization (Fig. 2d) indicated that about 2.8, 2.8, and 2.0% nitrogen were introduced to the graphene sheet for N-graphene (800), N-graphene (900), and N-graphene (1000), respectively. Based on the detailed analysis of N1s (Fig. 2e and Table 1), no obvious dependence of the ORR activity on the content of pyridine-like and pyrrole-like N species was observed. But this investigation showed that quaternary nitrogen atoms seem to be the most important species for the ORR due to the matching relationship between activity and quaternary N contents.[7,24] Thus any specific N species which resulted in the enhanced activity should not be selectively eliminated.

The electrochemical reduction of O_2 is a multi-electron reaction that has two main possible pathways: one is the transfer of two electrons to produce H_2O_2 and the other is a direct four-electron pathway to produce water. To obtain maximum energy capacity, it is highly desirable to reduce O_2 *via* the $4e^-$ pathway. Although the usual reaction that occurs on carbon electrodes is far less than the four-electron reaction, there have been reports that reactions involving more electrons may take place on nitrogen-containing carbon electrodes.[24–27] Herein, the selectivity of ORR was analyzed by two methods: RDE to obtain the slope of the Koutecky–Levich (K–L) plots and RRDE to direct the measurement of the portion of H_2O_2 formation *via* ring/disk current ratio. RRDE current–potential curves for N-graphene (900) at various rotating speeds are shown in Fig. 3a. Rotating rate-dependent limited diffusion currents were observed here. Fig. 3b shows the Koutecky–Levich (K–L) plots of $1/I_{lim}$ *vs.* $1/\omega^{1/2}$ at fixed potential (−0.5 V) on N-graphene (900) electrode derived from the data in Fig. 3a. The number of electrons calculated is 3.6, based on the K–L equation:

$$I_{lim} = 0.62nFD^{2/3}v^{-1/6}C_0\omega^{1/2} \quad (1)$$

where I_{lim} is the limiting current density, n is the number of electrons transferred per oxygen molecule, F is the Faraday constant (96 485 C mol^{-1}), D is the O_2 diffusion coefficient (1.73×10^{-5} cm^2 s^{-1}) in 0.1 M KOH, and C_0 is the concentration of oxygen (1.21×10^{-6} mol cm^{-3}).[28] To further verify the ORR pathways on the N-graphene (900), the formation of H_2O_2 during the ORR process was monitored using RRDE measurement. Analyses of the ORR by the reduction currents of the ring and disk (Fig. 3c and d) showed that the ORR on N-graphene (900) proceeds by a 3.8-electron reaction at −0.5 V to give about 10% of hydrogen peroxide according to the two equations:[29]

$$n = 4I_D/(I_D + (I_R/N)) \quad (2)$$

$$\%H_2O_2 = 100(4 - n)/2 \quad (3)$$

It is consistent with the data obtained from the slope of K–L plots. The results suggest that the ORR catalyzed on N-graphene (900) is a close $4e^-$ reduction process leading to the formation of H_2O.

Furthermore, the activity of N-graphene (900) for ORR was compared with commercial Pt/C electrocatalyst. From Fig. 4a, it can be seen that the two electrocatalysts have the same onset potentials and limited diffusion currents for oxygen reduction. In

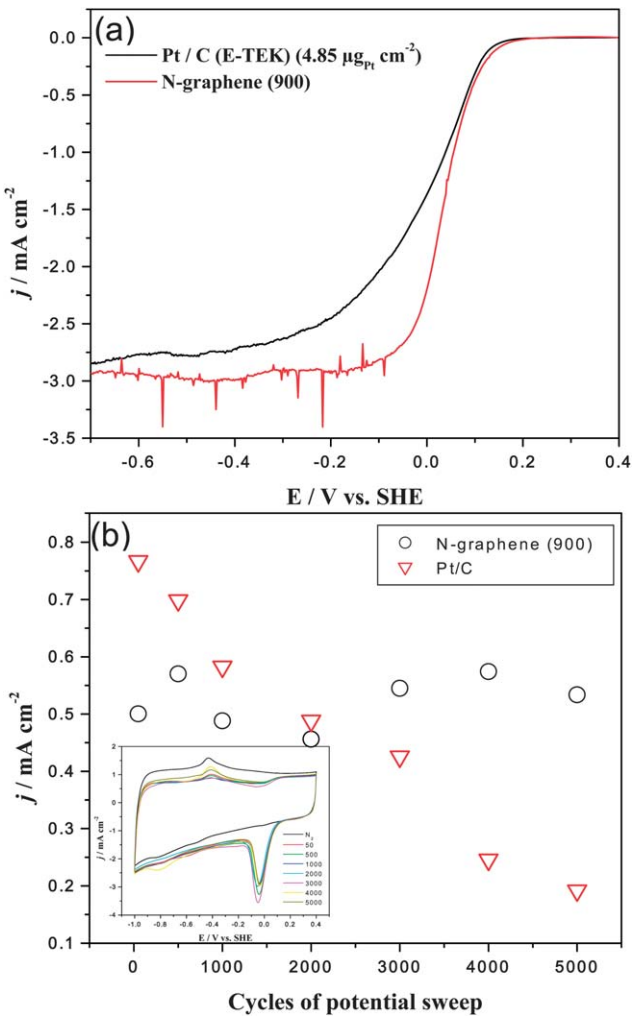

Fig. 4 (a) The polarization curves of oxygen reduction on N-graphene (900) and Pt/C (E-TEK) catalysts. Electrolyte: 0.1 M KOH, scan rate: 5 mV s^{-1}, and rotation speed: 1600 rpm. (b) Dependence of the current density for the ORR at 0.05 V on the potential cycles evaluated from the cyclic voltammograms of the inset. Inset: cyclic voltammograms of N-graphene (900) in N_2-saturated 0.1 M KOH (the black line) and O_2-saturated 0.1 M KOH after 50, 500, 1000, 2000, 3000, 4000, and 5000 potential cycles, respectively. Potential sweep rate: 100 mV s^{-1}.

addition, one can believe that N-graphene (900) has the slightly higher ORR activity than Pt/C (loading: 4.85 μg_{Pt} cm^{-2}) based on its half-wave potential (shifted positively about 43 mV).

A durability test of N-graphene (900) was also carried out by cyclic voltammetry in O_2-saturated 0.1 M KOH. The inset of Fig. 4b shows the CVs at various potential sweeps: 50, 500, 1000, 2000, 3000, 4000, and 5000 cycles. The cathodic peaks relate to the reduction of oxygen. Almost no change in the voltammetric charge was found after 5000 cycles of the potential sweep. In Fig. 4b, the dependence of the current density for the ORR on the potential cycles is presented based on the data from the inset. Clearly, the ORR current density on N-graphene (900) electrode remains stable. In contrast, the ORR current density on Pt/C electrode, subjected to an identical test (CV data not shown), has a rapid decline. N-graphene (900) thus demonstrated better durability than Pt/C under the studied conditions.

4. Conclusions

It is clearly shown here that nitrogen-doped graphene catalysts can be synthesized by the treatment of graphene by ammonia under different temperatures. The highest ORR activity in alkaline solution was obtained with the catalyst treated at 900 °C. XPS indicated that only 2.8% nitrogen was introduced into the graphene for N-graphene (900). Quaternary type nitrogen species seem to play the most important role for ORR activity. Moreover, our electrochemical measurements showed that N-graphene (900) catalysts promote the desired $4e^-$ ORR in alkaline solution. In comparison to the commercial Pt/C catalyst, N-graphene (900) catalyst presented higher ORR onset potential (0.308 V) and 43 mV more positive ORR half-wave potential. Also importantly, it demonstrated better stability than Pt/C (loading: 4.85 μg_{Pt} cm^{-2}) in the studied conditions. Therefore, N-doped graphene may have the potential to replace the costly Pt/C catalyst in fuel cells in an alkaline solution.

Acknowledgements

This research was supported by Natural Sciences and Engineering Research Council of Canada (NSERC), Ballard Power Systems Inc., Canada Research Chair (CRC) Program, Canada Foundation for Innovation (CFI), Ontario Research Fund (ORF), Ontario Early Researcher Award (ERA) and the University of Western Ontario.

References

1 M. Lefèvre, E. Proietti, F. Jaouen and J.-P. Dodelet, *Science*, 2009, **324**, 71.
2 B. Winther-Jensen, O. Winther-Jensen, M. Forsyth and D. R. MacFarlane, *Science*, 2008, **321**, 671.
3 J. Zhang, K. Sasaki, E. Sutter and R. R. Adzic, *Science*, 2007, **315**, 220.
4 H. A. Gateiger, S. S. Kocha, B. Sompalli and F. T. Wagner, *Appl. Catal., B*, 2005, **56**, 9.
5 R. Liu, D. Wu, X. Feng and K. Müllen, *Angew. Chem., Int. Ed.*, 2010, **49**, 2565.
6 T. C. Nagaiah, S. Kundu, M. Bron, M. Muhler and W. Schuhmann, *Electrochem. Commun.*, 2010, **12**, 338.
7 N. P. Subramanian, X. Li, V. Nallathambi, S. P. Kumaraguru, H. Colon-Mercado, G. Wu, J.-W. Lee and B. N. Popov, *J. Power Sources*, 2009, **188**, 38.
8 Y. Tang, B. L. Allen, D. R. Kauffman and A. Star, *J. Am. Chem. Soc.*, 2009, **131**, 13200.
9 K. Prehn, A. Warburg, T. Schilling, M. Bron and K. Schulte, *Compos. Sci. Technol.*, 2009, **69**, 1570.
10 K. Gong, F. Du, Z. Xia, M. Durstock and L. Dai, *Science*, 2009, **323**, 760.
11 T. Iwazaki, R. Obinata, W. Sugimoto and Y. Takasu, *Electrochem. Commun.*, 2009, **11**, 376.
12 M. Lefèvre, J. P. Dodelet and P. Bertrand, *J. Phys. Chem. B*, 2002, **106**, 8705.
13 A. L. Bouwkamp-Wijnoltz, W. Visscher, J. A. R. van Veen, E. Boellaard, A. M. van der Kraan and S. C. Tang, *J. Phys. Chem. B*, 2002, **106**, 12993.
14 M. J. Allen, V. C. Tung and R. B. Kaner, *Chem. Rev.*, 2010, **110**, 132.
15 A. K. Geim, *Science*, 2009, **324**, 1530.
16 K. I. Bolotin, K. J. Sikes, Z. Jiang, M. Klima, G. Fudenberg, J. Hone, P. Kim and H. L. Stormer, *Solid State Commun.*, 2008, **146**, 351.
17 A. K. Geim and K. S. Novoselov, *Nat. Mater.*, 2007, **6**, 183.
18 M. D. Stoller, S. Park, Y. Zhu, J. An and R. S. Ruoff, *Nano Lett.*, 2008, **8**, 3498.
19 D. A. Stevens, M. T. Hicks, G. M. Haugen and J. R. Dahn, *J. Electrochem. Soc.*, 2005, **152**, A2309.
20 L. Qu, Y. Liu, J.-B. Baek and L. Dai, *ACS Nano*, 2010, **4**, 1321.
21 H. C. Schniepp, J.-L. Li, M. J. McAllister, H. Sai, M. Herrera-Alonso, D. H. Adamson, R. K. Prud'homme, R. Car, D. A. Saville and I. A. Aksay, *J. Phys. Chem. B*, 2006, **110**, 8535.
22 X. Li, H. Wang, J. T. Robinson, H. Sanchez, G. Diankov and H. Dai, *J. Am. Chem. Soc.*, 2009, **131**, 15939.
23 D. Geng, H. Liu, Y. Chen, R. Li, X. Sun, S. Ye and S. Knights, *J. Power Sources*, 2011, **196**, 1795.
24 T. Iwazaki, H. Yang, R. Obinata, W. Sugimoto and Y. Takasu, *J. Power Sources*, 2010, **195**, 5840.
25 P. H. Matter, E. Wang, M. Arias, E. J. Biddinger and U. S. Ozkan, *J. Mol. Catal. A: Chem.*, 2007, **264**, 73.
26 J.-I. Ozaki, N. Kimura, T. Anahara and A. Oya, *Carbon*, 2007, **45**, 1847.
27 R. A. Sidik, A. B. Anderson, N. P. Subramanian, S. P. Kumaraguru and B. N. Popov, *J. Phys. Chem. B*, 2006, **110**, 1787.
28 R. E. Davis, G. L. Horvath and C. W. Tobias, *Electrochim. Acta*, 1967, **12**, 287.
29 U. A. Paulus, T. J. Schmidt, H. A. Gasteiger and R. J. Behm, *J. Electroanal. Chem.*, 2001, **495**, 134.